Design Criteria for a Wide Input/Output Range LLC Converter Using Topological Reconfigurations

Takashi Ohno
Dept. of Science of Technology Innovation
Nagaoka University of Technology
Nagaoka, Japan
s225058@stn.nagaoka.ut.ac.jp

Guillaume Lefevre
Dept. of Power Electronic Systems
Mitsubishi Electric R&D Centre Europe
Rennes, France
G.Lefevre@fr.merce.mee.com

Guillaume Regnat
Dept. of Power Electronic Systems
Mitsubishi Electric R&D Centre Europe
Rennes, France
G.Regnat@fr.merce.mee.com

Davide Barlini
Dept. of Power Electronic Systems
Mitsubishi Electric R&D Centre Europe
Rennes, France
D.Barlini@fr.merce.mee.com

Hiroki Watanabe
Dept. of Electrical, Electronics, and Information Engineering
Nagaoka University of Technology
Nagaoka, Japan
hwatanabe@vos.nagaokaut.ac.jp

Jun-ichi Itoh
Dept. of Science of Technology Innovation
Nagaoka University of Technology
Nagaoka, Japan
itoh@vos.nagaokaut.ac.jp

***Abstract*— This paper proposes a circuit design methodology for an LLC converter capable of a wide input and output voltage range. By utilizing the full-bridge and the half-bridge switching configurations, the proposed converter achieves a 19% reduction in transformer volume and a 65% reduction in resonance inductor volume compared to a conventional full-bridge LLC converter. The converter maintains zero-voltage switching under all operation voltages and load conditions, using the proposed design methodology. Finally, the FB/HB LLC converter demonstrated a maximum efficiency of 94.2%.**

Keywords—wide range, zero voltage switching, LLC converter, design methodology

I. INTRODUCTION

Recently, Inductor-Inductor-Capacitor (LLC) resonant converters have been widely applied in battery chargers due to their high efficiency, compact size, and low noise characteristics [1]. To accommodate the varying battery voltage that depends on the state of charge (SOC), the associated DC-DC converter must operate over a wide voltage range. However, applying LLC converters under such wide voltage conditions presents challenges, including increased component volume and reduced efficiency [2].

To address these issues, various circuit reconfiguration techniques have been proposed to improve conversion efficiency over a wide voltage range [3]–[6]. Two-stage [3], multilevel [4], interleaved [5], and auxiliary circuit [6] technologies have been demonstrated to improve the performance. However, these circuit reconfiguration technologies inevitably increase the number of components, leading to reduced power density and increased cost.

Control strategies have also been investigated to improve efficiency across a broad operating range [7][8]. For example, phase-shift control [7] extends the operation range by adjusting the phase angle between the inverter legs. However, excessive phase-shift angle cannot compromise zero voltage switching (ZVS) due to the reduction in magnetizing current. Furthermore, a time domain analysis (TDA) model is required because the inverter voltage in phase-shift control deviates significantly from a sinusoidal wave. This increases the complexity of both the design and optimization process. Burst mode control, which adjusts the burst duty ratio to extend the buck gain [8], requires large capacitors to suppress low-frequency ripple voltage.

Recently, full-bridge and half-bridge (FB/HB) mode switching control techniques have been proposed to expand the voltage gain range by more than two times [9][10][11]. In [9], an on-the-fly control strategy is introduced to avoid output-voltage fluctuations during the mode transition between FB and HB modes. However, DC offset and asymmetric transformer current may cause higher peak current and lead to saturation. In other words, the transformer should be designed to avoid saturation during mode transitions which may result in an oversized transformer. In [10], the DC component of the transformer is eliminated by employing a symmetric-duty control during mode transition.

As another mode-transition method, [11] proposed state plane-based topology morphing control (SPTMC). In SPTMS the frequency variation at the mode transition is predicted in advance and feedforward to the controller to optimize the dynamic response. Thus, several studies have focused on mode-transition techniques.

However, the parameter-design methodologies in these studies follow the conventional LLC converter design process. In other words, these articles cannot be regarded as design methods developed for FB and HB operation. In practice, one operating range is set to fully include the other. The mode-transition point is specified at the point where the maximum voltage in FB mode equals the minimum voltage in HB mode.

This paper proposes a practical design methodology for a wide-range LLC converter utilizing FB/HB switching control. The objective is to ensure ZVS across the entire operating range while minimizing the volume of magnetic components.

The key new contribution of this paper is to provide a simple design methodology based on the first harmonic approximation (FHA) model [12]. This model enables the designer to predetermine the magnetic materials and switching devices by limiting the switching frequency within specific bounds. Furthermore, the transition between FB and HB mode is determined by taking into account both the voltage and the load conditions. Consequently, the operating voltage range for the design process of the FB mode is minimized. The effectiveness of the proposed methodology is demonstrated through downsizing analysis of both the transformer and the resonant inductor, and experimental validation using a 1.5-kW prototype.

II. Circuit Configuration and Control Strategy

Fig. 1 shows the circuit configuration of the FB/HB LLC converter, consisting of a full-bridge inverter, a resonant tank, and a diode rectifier. The appropriate operating mode, either full-bridge or half-bridge, is selected depending on the input voltage and load conditions to ensure optimal performance.

Fig. 2 shows the steady-state waveforms of each operation mode. In Fig. 2(a), the primary inverter generates a square waveform of $\pm V_{in}$, with all switching devices operating at a 50% duty ratio. In Fig. 2(b), the primary inverter generates a square waveform from 0 V to V_{in} by operating S_1 and S_2 at a 50% duty ratio, turning off S_3, and keeping S_4 continuously turned on. The resonant capacitor blocks the DC offset in the inverter output.

III. Parameter Design Steps and Volume Evaluation

The design methodology for the LLC converter is based on the FHA model. ZVS is achieved across the entire operating range. The minimum and the maximum switching frequencies are defined as initial design parameters.

A. FHA Model

Fig. 3 shows the equivalent circuit of the LLC converter, which is converted to the primary side. The equivalent output resistance is expressed as

$$R_{ac} = \frac{8N_{Tr}^{\ 2}}{\pi^2} R_o \quad (1),$$

Where N_{Tr} is the transformer turns ratio and Ro is the load resistance, varying with the output voltage and power.

From Fig. 3, the voltage gain of the conventional FHA model is expressed as a function of the quality factor, the inductance ratio, and the normalized frequency as

$$M_{FHA} = \frac{1}{\sqrt{\left(1+\lambda-\frac{\lambda}{f_n^{\ 2}}\right)^2 + Q^2\left(f_n-\frac{1}{f_n}\right)^2}} \quad (2),$$

where $\lambda(L_r/L_m)$ is the inductance ratio, f_n (f_S/f_r) is the normalized switching frequency, and Q is the quality factor.

Fig. 4 shows the voltage gain characteristics of the LLC converter based on the FHA model. The LLC converter operates as an inductive region when the normalized frequency is higher than 1.0, which corresponds to the resonant frequency determined by C_r and L_r. In contrast, the LLC converter operates with inductive or capacitive characteristics depending on the load condition when the normalized frequency is less than 1.0. In the capacitive region, the LLC converter operates with zero current switching (ZCS). The LLC converter operates with ZVS in the inductive region, which is generally designed to operate with ZVS. The boundary condition between the inductive and capacitive regions is expressed as

$$M_{ZVS} = \frac{f_n}{\sqrt{f_n^{\ 2}(1+\lambda)-\lambda}} \quad (3).$$

(3) defines the boundary condition, in which the operating point (specified by the load condition and voltage gain) operates to ZVS operation when voltage gain is above M_{ZVS}, whereas ZCS operation occurs when voltage gain is below M_{ZVS}.

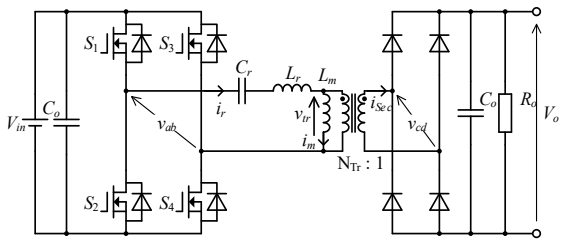

Fig. 1. Circuit configuration of the FB/HB LLC converter. The LLC converter consists of a full-bridge inverter, a resonant tank, and a full-bridge rectifier.

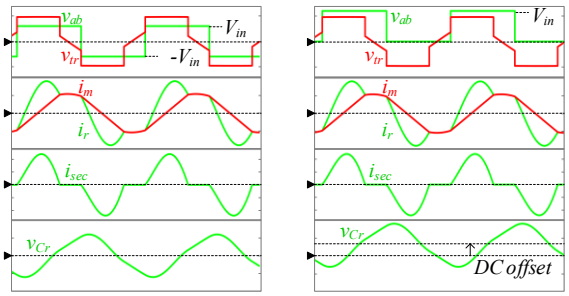

(a) Full-Bridge mode (b) Half-Bridge mode

Fig. 2. Operation waveform of each operation mode. In FB mode, pulse-minus input voltage, $\pm V_{in}$ is applied to the resonant tank. On the other hand, in the HB mode, the full-bridge inverter outputs a voltage from zero to $+V_{in}$.

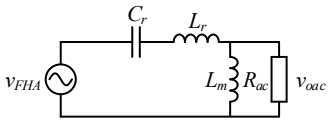

Fig. 3. Equivalent circuit of the LLC converter, which is converted to the primary side. Also, the square waveform of the inverter output voltage is approximated by a sine wave, which is the dundamental waveform.

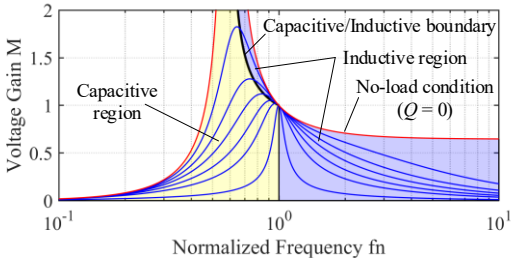

Fig. 4. The voltage gain characteristics of the LLC converter based on the FHA model. If the normalized frequency, f_n is higher than 1.0, the LLC converter operates in ZVS. If the f_n is less than 1.0, the LLC converter operates ZVS or ZVS, depending on the voltage gain and load conditions.

B. Parameter Design Steps

Fig. 5 shows the design steps of the wide-range LLC converter. In this design steps, the following parameters need to be given as initial parameters.

- Min./Max. input voltage: V_{inmin}, V_{inmax}
- Min./Max. output voltage: V_{omin}, V_{omax}
- Min./Max. switching frequency: f_{Smin}, f_{Smax}
- Rated power: P_{max}
- Transformer turns ratio: N_{Tr}

- Max. input voltage of the FB mode: $V_{inFBmax}$
- Dead time: t_d
- Output capacitance of the MOSFET: C_{oss}

Step 1. Max./min. voltage gain: The max. and the min. voltage gain of the LLC converter is defined as

$$M_{\min(\max)} = \frac{N_{Tr} V_{o\min(\max)}}{V_{in\max(\min)}} \quad (4).$$

The voltage gain is calculated by referring to the primary side. Thus, the output voltage is multiplied by the transformer turns ratio, N_{tr}.

Step 2. Determination of resonant frequency: The LLC converter achieves ZVS at both the minimum gain with maximum frequency and the maximum gain with minimum frequency. The inductance ratio required to achieve the

minimum gain at the maximum frequency is derived by substituting $Q = 0$ into (2).

$$\lambda = \frac{1 - M_{\min}}{M_{\min}} \frac{{f_{n\max}}^2}{{f_{n\max}}^2 - 1} \quad (5),$$

where f_{nmax} is the maximum normalized frequency.

From (3) and (5), the resonant frequency is calculated as

$$f_r = f_{S\min} f_{S\max} \sqrt{\frac{\frac{1 - M_{\min}}{M_{\min}} + \frac{{M_{\max}}^2 - 1}{{M_{\max}}^2}}{\frac{1 - M_{\min}}{M_{\min}} {f_{S\max}}^2 + \frac{{M_{\max}}^2 - 1}{{M_{\max}}^2} {f_{S\min}}^2}} \quad (6).$$

By setting the inductance ratio, λ and the resonant frequency, f_r according to (5) and (6), ZVS is ensured at the maximum load and maximum gain. In addition, under the no-load and minimum gain conditions, the LLC converter operates at the maximum switching frequency.

Step 3. Normalized frequency definition: The maximum and minimum normalized frequency are expressed as

$$f_{n\max(\min)} = \frac{f_{S\max(\min)}}{f_r} \quad (7),$$

where f_{nmin} is the minimum normalized frequency.

Step 4. Inductance ratio: The inductance ratio of the LLC converter is calculated from (5).

Step 5. Min. characteristic impedance: The boundary condition of the characteristic impedance to obtain the required voltage gain is expressed as

$$z_0(V_o) = R_{ac} Q = \frac{8\lambda V_{in\min} N_{Tr} V_o}{\pi^2 P_{\max}} \sqrt{\frac{1}{\lambda} + \frac{(N_{Tr} V_o)^2}{(N_{Tr} V_o)^2 - {V_{in\min}}^2}} \quad (8).$$

Fig. 6 shows the boundary condition of the characteristic impedance to obtain the required voltage gain at the maximum power and the relationship between the normalized max. voltage gain and the output voltage. The characteristic impedance of the LLC converter should be selected lower than the min. boundary condition to satisfy the voltage gain all output voltage ranges. Note that the min. the boundary condition is not defined at the min. output voltage.

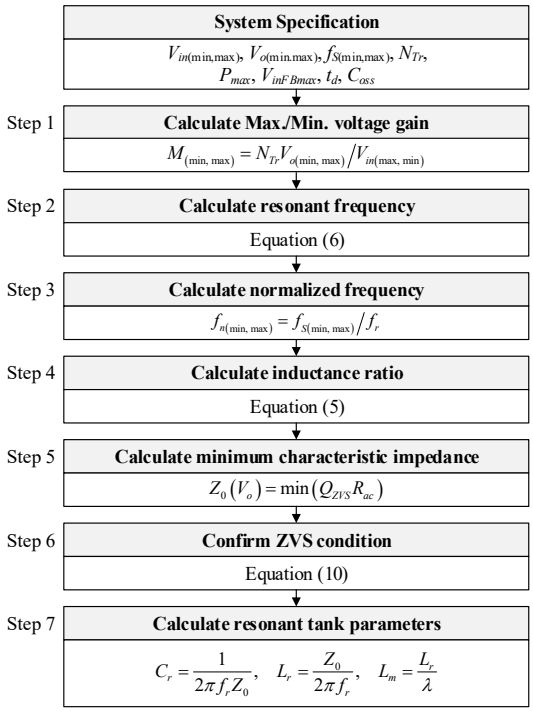

Fig. 5. Parameter design procedure for wide range LLC converter.

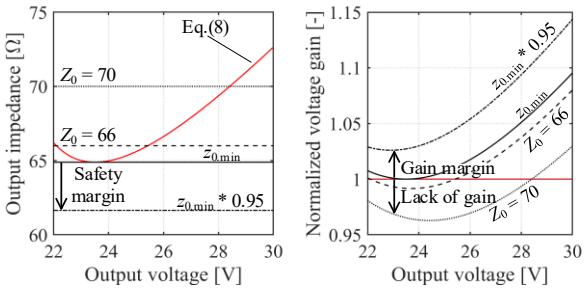

(a) Characteristic impedance (b) Gain characteristics

Fig. 6. Characteristic impedance and gain characteristics. The operation range of the LLC converter is guaranteed by designing the LC tank using the lowest characteristic impedance.

Fig. 6(b) shows the relationship between the normalized max. voltage gain and the output voltage. If the resonant tank is designed using characteristic impedance of z_{0min}, the voltage gain of the LLC converter satisfies the system specification at all output voltage ranges. On the other hand, if the resonant tank is selected using the characteristic impedance of 66 Ω, the voltage gain is satisfied at 22 V and 30 V. However, the voltage gain is not enough at around 24 V. Therefore, the characteristic impedance of the resonant tank is calculated as

$$Z_0 = \min\left(z_0(R_o)\right) \times 0.95 \quad (9),$$

where 0.95 is the safety margin of the design.

Step 6. Verification of the ZVS condition considering parasitic capacitance: The ZVS condition considering parasitic capacitance [12] is expressed as

$$Z_0 \le \frac{2}{\pi} \frac{\lambda {f_{n\max}}^2}{(\lambda + 1){f_{n\max}}^2 - \lambda} \frac{t_d}{C_{ZVS}} \quad (10),$$

where C_{ZVS} is the sum of the output capacitance of the upper and lower switching devices and the parasitic capacitance between GND and the resonant tank.

Step 7. Resonant tank parameters: Finally, using the calculated characteristic impedance, the resonant tank parameters are calculated as

$$C_r = \frac{1}{2\pi f_r Z_0} \quad (11),$$

$$L_r = \frac{Z_0}{2\pi f_r} \quad (12),$$

$$L_m = \frac{L_r}{\lambda} \quad (13),$$

where C_r is the resonant capacitance, L_r is the resonant inductance, L_m is the magnetizing inductance.

C. Evaluation of the magnetic component volume.

The transformer volume and the resonant inductor volume are evaluated based on the area product (AP) method [13]. The AP is calculated based on the electrical constraints (voltage-time product, root mean square (RMS) current, and peak current), maximum flux density, current density of the winding, and winding factor. Additionally, the AP does not depend on the number of turns in the magnetic components.

Using Faraday's law and the relationship between RMS current and current density, the AP is calculated as

$$AP_{Tr} = A_{CTr} A_{WTr} = \frac{k_w}{4} \frac{N_{Tr} V_o}{B_{\max} f_{eq}} \left(\frac{I_r + I_{\sec}/N_{Tr}}{J_{\max}} \right) \quad (14),$$

where A_{CTr} is the core cross-section area of the transformer, A_{WTr} is the winding cross-section area of the transformer, k_w is the winding factor, B_{max} is the max. flux density, f_{eq} is the equivalent frequency, I_r is the RMS current of the resonant tank, I_{sec} is the RMS current of the secondary side, and J_{max} is the max. current density of the winding.

Fig. 7 shows the relationship between transformer voltage and flux density. The transformer voltage waveform is approximated as shown in Fig. 7(a) in the boost region ($f_S < f_r$). In contrast, the transformer voltage waveform is shown in Fig. 7(b) in the buck region ($f_S > f_r$) of the LLC converter. Therefore, the equivalent frequency in (14) is expressed as

$$f_{eq} = \begin{cases} f_r & [f_r \geq f_S] \\ f_S & [f_r < f_S] \end{cases} \quad (15).$$

Similarly, the AP of the resonant inductor is calculated as

$$AP_{Lr} = A_{CLr} A_{WLr} = k_w \frac{L_r I_{rPk} I_r}{B_{\max} J_{\max}} \quad (16),$$

where A_{CLr} is the core cross-section area of the resonant inductor and A_{WLr} is the winding cross-section area of the resonant inductor.

Also, the relationship between the AP and the magnetic components volume is expressed as

$$Vol = k_{geom} \left(A_C A_W \right)^{\frac{3}{4}} \quad (17),$$

where k_{geom} is the geometrical factor which varies depending on the core materials and the core shape.

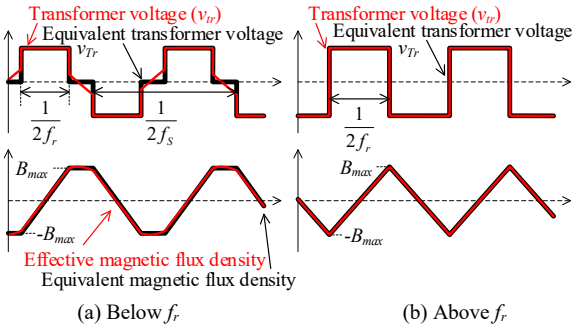

Fig. 7. Relationship between transformer voltage and flux density. If the switching frequency, f_S is smaller than the resonant frequency, f_r, the transformer voltage is approximated as a three-level waveform. Therefore, the voltage-time product is calculated using the resonant frequency at the $f_S < f_r$ condition.

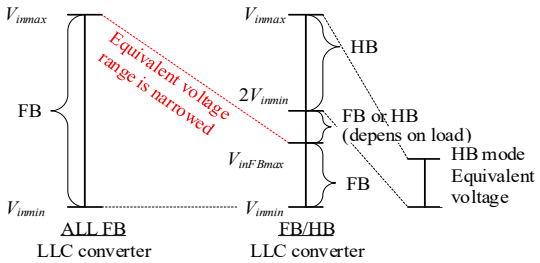

Fig. 8. Design image for each control strategy. The FB mode at input voltage, V_{in} and the HB mode at two times V_{in} have the same operating characteristics because the amplitude applied to the resonant tank is completely the same.

TABLE I. SPECIFICATION OF LLC CONVERTER

Element	Symbol	ALL FB	FB/HB
Input voltage [V]	V_{in}	300 – 800	
Output voltage [V]	V_{out}	22 – 30	
Max. input voltage of FB mode [V]	$V_{inFBmin}$	800	450
Max. output power [kW]	P_{max}	1.5	
Switching frequency [kHz]	f_S	200 – 600	
Transformer turns ratio [-]	N_{Tr}	16	
Dead time [ns]	t_d	150	
Output capacitance [pF]	C_{oss}	65	
Max. current density [A/cm^2]	J_{max}	400	
Max. magnetic flux density [Wb/cm^2]	B_{max}	1.5×10^{-5}	
Winding factor	k_w	3	

In practice, k_{geom} is therefore extremely difficult to determine its exact value. For this reason, this paper does not refer to specific value of k_{geom}, but instead performs only a relative evaluation between the ALL-FB LLC converter and the FB/HB LLC converter.

D. Parameter design of the LLC converter

Fig. 8 shows the design image of the ALL FB LLC converter and FB/HB LLC converter. The ALL FB converter operates in FB mode only across all voltage ranges. In contrast the equivalent input voltage range of the FB/HB LLC converter is narrowed using the HB mode.

Table I shows the specifications of the LLC converters. The ALL FB LLC converter operates with the input voltage from 300 V to 800 V in FB mode only. The FB/HB LLC

converter operates with the input voltage range from 300 V to 450 V in the FB mode, from 600 V to 800 V in the HB mode, and from 450 V to 600 V by switching operation between the FB and the HB modes depending on the load conditions.

Fig. 9 shows the voltage gain characteristics of the LLC converter. Fig. 9(a) shows the voltage gain characteristics of the ALL FB LLC converter, which obtains the required gain at the rated power condition. Also, the min. voltage gain at the no-load condition is obtained at the max. switching frequency. Fig. 9(b) shows the voltage gain characteristic of the FB/HB LLC converter, which similarly obtains the required voltage gain using the FB and the HB modes.

Table II shows the designed parameters of the ALL FB LLC converter and the FB/HB LLC converter. Using the HB mode, the AP of the transformer is reduced by 25% from 1.57 cm^4 to 1.18 cm^4. From the (17), the transformer volume is reduced by 19%. Similarly, the resonant inductor AP is reduced by 75% from 1.73 cm^4 to 0.431 cm^4. The volume of the resonant inductor is reduced by 65%.

IV. Experimental Verification

The prototype consists of the primary inverter, the resonant tank, and the secondary diode rectifier. The switching device of the primary side is SiC MOSFETs (C3M0160120J, Wolfspeed). The secondary diode is Trench MOS Barrier Schottky (V60D60C, Vishay), which uses two in parallel on each arm.

A. Experimental waveforms

Fig. 10 shows the operation waveforms of the FB/HB LLC converter. Fig. 10(a) shows the operating waveform of the FB mode, which is the input voltage of 300 V, the output voltage of 30 V, and the output power of 1.5 kW. The primary inverter outputs a square waveform of $\pm V_{in}$. Also, the converter operates at a switching frequency of 223 kHz, which closely matches the 215 kHz predicted by the FHA model, with a deviation of only 3.6%. Although the use of the FHA model introduces some approximation error in the proposed design methodology, the error remains sufficiently small. Furthermore, the switching frequency observed in the experiment is higher than the calculated value by the FHA model, which remains within the specified frequency range, resulting in no practical issues.

Fig. 10(b) shows the HB mode, which is the input voltage of 600 V, the output voltage of 30 V, and the output power of 1.5 kW. The primary inverter outputs a square waveform of 0 to $+V_{in}$. The transformer does not apply a DC component because the DC offset in the HB mode is blocked by the resonant capacitor. Additionally, the ZVS of the LLC converter is achieved at the rated power.

Fig. 11 shows the operation waveforms of the no-load condition at the input voltage of 450 V, the output voltage of 22 V, and the switching frequency of 600 kHz. The proposed parameter design methodology is designed to achieve ZVS under no-load conditions, which is confirmed by the experimental waveform.

B. Efficiency characteristics

Fig. 12(a) shows the efficiency characteristics of the FB and HB modes. In the FB mode, the experimental conditions are an input voltage of 300 V and an output voltage of 30 V, which corresponds to the maximum voltage-gain condition.

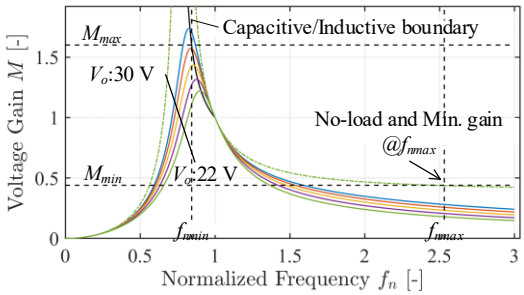

(a) ALL FB LLC converter

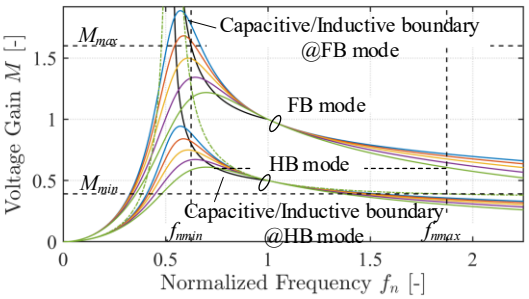

(b) FB/HB LLC converter

Fig. 9. Gain characteristics of each control strategy. Both gain characteristics are designed to achieve maximum and minimum voltage gain.

TABLE II. Designed Parameter of the LLC Converter

Element	Symbol	ALL FB	FB/HB
Resonant inductance [μH]	L_r	107	25.8
Magnetizing inductance [μH]	L_m	71.0	66.3
Resonant capacitance [nF]	C_r	4.21	9.56
Transformer area product [cm^4]	AP_{Tr}	1.57	1.18
Inductor area product [cm^4]	AP_{Lr}	1.73	0.431

In the HB mode, the converter operates with an input voltage of 600 V and an output voltage of 30 V. Under these HB mode conditions, the equivalent voltage is the same as that of the 300 V input condition in the FB mode. The maximum efficiency is 93.6% at an output power of 900W in HB mode. In both FB and HB operating modes, the LLC converter demonstrated similar efficiency characteristics.

Fig. 12(b) shows the efficiency characteristics of the input voltage. The LLC converter operates in FB mode from 300 V to 600 V, and in HB mode from 600 V to 800 V. At the rated power condition, the maximum efficiency of 94.2% is obtained at an input voltage of 450 V.

V. Conclusion

This paper discusses the parameter design methodology for the wide range LLC converter using the FB and the HB modes. The result of the comparison with the ALL FB LLC converter is that the volume of the FB/HB LLC converter is reduced by 19% for the transformer and 65% for the resonant inductance. Furthermore, the validity of the design methodology is demonstrated by confirming the ZVS at the rated power and no-load conditions.

References

[1] J. -I. Baek, J. -K. Kim, J. -B. Lee, H. -S. Youn and G. -W. Moon, "A Boost PFC Stage Utilized as Half-Bridge Converter for High-

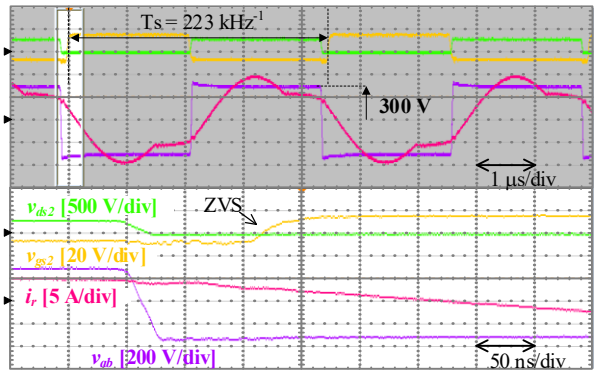

(a) Full bridge mode @ V_{in}: 300 V, V_o: 30 V, R_o: 0.6 Ω

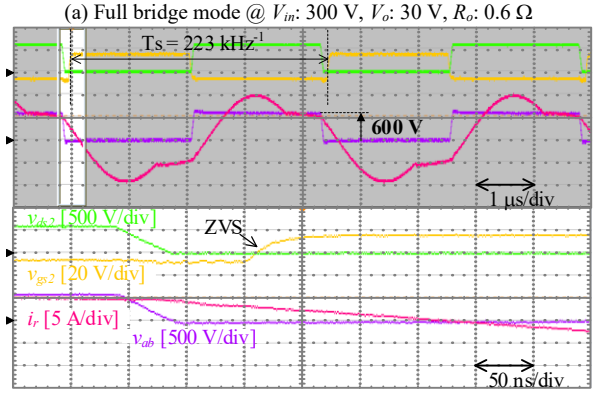

(b) Half bridge mode @ V_{in}: 600 V, V_o: 30 V, R_o: 0.6 Ω

Fig. 10. Operation waveforms at rated power. The experimental waveforms are the most boosting operating conditions in FB and HB modes. The same characteristics are obtained for FB and HB asa per the design concept. Also, the LLC converter achieved ZVS at the maximum boost condition and rated power.

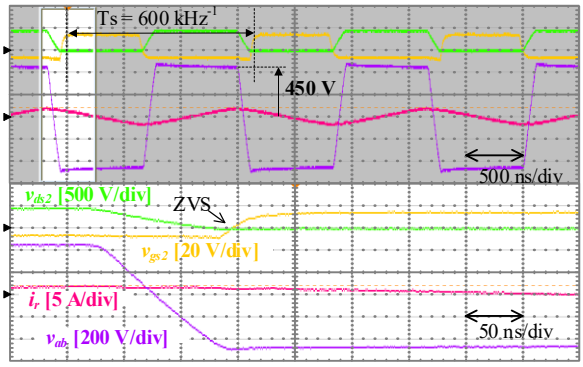

Fig. 11. Operation waveforms under the lowest voltage gain and no-load conditions. The proposed design parameters are verified to ensure the ZVS condition even under no-load conditions.

Efficiency DC–DC Stage in Power Supply Unit," in IEEE Transactions on Power Electronics, vol. 32, no. 10, pp. 7449-7457, Oct. 2017

[2] W. Inam, K. K. Afridi and D. J. Perreault, "Variable Frequency Multiplier Technique for High-Efficiency Conversion Over a Wide Operating Range," in IEEE Journal of Emerging and Selected Topics in Power Electronics, vol. 4, no. 2, pp. 335-343, June 2016

[3] C. Fei, M. H. Ahmed, F. C. Lee and Q. Li, "Two-Stage 48 V-12 V/6 V-1.8 V Voltage Regulator Module With Dynamic Bus Voltage Control for Light-Load Efficiency Improvement," in IEEE Transactions on Power Electronics, vol. 32, no. 7, pp. 5628-5636, July 2017

[4] X. Wu, R. Li and X. Cai, "A Wide Output Voltage Range LLC Resonant Converter Based on Topology Reconfiguration Method," in

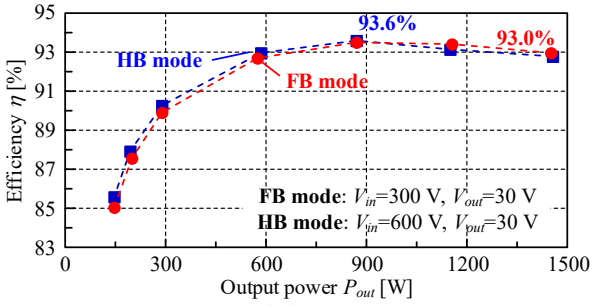

(a) Load characteristics

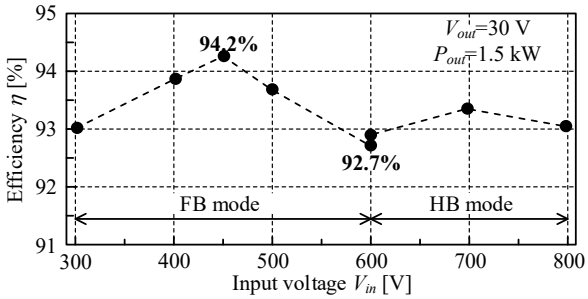

(a) Input-voltage characteristics at the rated power.

Fig. 12. Load and input voltage efficiency characteristics. The load characteristics are compared between the FB and HB modes under the condition where the equivalent voltages are identical. In the input-voltage characteristics, the LLC converter operates in FB mode from 300 V to 600 V, and in HB mode from 600 V to 800 V.

IEEE Journal of Emerging and Selected Topics in Power Electronics, vol. 10, no. 1, pp. 969-983, Feb. 2022

[5] H. Wu, X. Zhan and Y. Xing, "Interleaved LLC Resonant Converter With Hybrid Rectifier and Variable-Frequency Plus Phase-Shift Control for Wide Output Voltage Range Applications," in IEEE Transactions on Power Electronics, vol. 32, no. 6, pp. 4246-4257, June 2017

[6] J. Wu, S. Li, S. -C. Tan and S. Y. R. Hui, "Fixed-Frequency Phase-Shift Modulated Capacitor-Clamped LLC Resonant Converter for EV Charging," in IEEE Transactions on Power Electronics, vol. 37, no. 11, pp. 13730-13742, Nov. 2022

[7] I. Kim, W. -Y. Jang, S. -J. Lee and J. -W. Park, "Enhanced PFM-PSM Hybrid Control of CLLC Resonant Converter for Electric Vehicles: Comprehensive Study and Verification," in IEEE Transactions on Power Electronics, vol. 39, no. 10, pp. 12978-12990, Oct. 2024

[8] L. Shi, B. Liu and S. Duan, "Burst-Mode and Phase-Shift Hybrid Control Method of LLC Converters for Wide Output Range Applications," in IEEE Transactions on Industrial Electronics, vol. 67, no. 2, pp. 1013-1023, Feb. 2020

[9] M. M. Jovanović and B. T. Irving, "On-the-Fly Topology-Morphing Control—Efficiency Optimization Method for LLC Resonant Converters Operating in Wide Input- and/or Output-Voltage Range," in IEEE Transactions on Power Electronics, vol. 31, no. 3, pp. 2596-2608, March 2016

[10] J. Chen,

[11] J. Chen, J. Xu and Y. Wang, "Seamless Control of Full-Bridge and Halidge Topology Morphing LLC Converter Based on State Plane Analysis," in IEEE Transactions on Power Electronics, vol. 39, no. 1, pp. 198-211, Jan. 2024

[12] S. D. Simone, “LLC resonant half-bridge converter design guideline,” STMicroelectronics, 2014. [Online]. Available. https://www.st.com/content/ccc/resource/technical/document/application_note/31/fb/59/5e/93/8c/42/b9/CD00143244.pdf/files/CD00143244.pdf/jcr:content/translations/en.CD00143244.pdf

[13] W. T. Mclyman, Transformer and Inductor design Handbook. California, U.S.A. Kg Magnetics, Inc, 2011.